Article

Bioconversion of a Peanut Oil Processing By-Product into a Novel *α*-Glucosidase Inhibitor: Hemi-Pyocyanin

Van Bon Nguyen [1] **, San-Lang Wang** [2,3,*] **and Anh Dzung Nguyen** [1,*]

1   Institute of Biotechnology and Environment, Tay Nguyen University, Buon Ma Thuot 630000, Vietnam; nvbon@ttn.edu.vn
2   Department of Chemistry, Tamkang University, New Taipei City 25137, Taiwan
3   Life Science Development Center, Tamkang University, New Taipei City 25137, Taiwan
*   Correspondence: sabulo@mail.tku.edu.tw (S.-L.W.); nadzung@ttn.edu.vn (A.D.N.)

Abstract: Hemi-pyocyanin (HPC) is a heterocyclic nitrogenous compound with some reported potential medical effects. The current report aimed to investigate the potential use of organic industrial waste for the production of HPC via microbial fermentation. The novel antidiabetic activity of HPC was also accessed and reported in this work. A peanut oil processing by-product (groundnut cake) was screened as the best substrate for *Pseudomonas aeruginosa* TUN03 conversion to obtain high-yield HPC. This compound was further produced in a 14 L bioreactor system on a large scale (6 L per pilot) and reached higher productivity (35.1 µg/mL) in a shorter time course of cultivation (8 h) compared to fermentation on a small scale in flasks (19.5 µg/mL; 3 days of fermentation). On assessing its activity, HPC demonstrated potent inhibition against α-glucosidase, an antidiabetic enzyme, with a low IC50 value (0.572 mg/mL) and a maximum inhibition rate of 100%. In an in silico study, HPC was found to inhibit α-glucosidase with a good binding energy score (−9.0 kcal/mol) via interaction with amino acids Lys156, Leu313, and Arg315 at the active site, and three bonds (1 H-acceptor and 2 pi-H) were generated. The data from five Lipkin's rules and ADMET-based pharmacokinetics and pharmacology revealed that HPC possesses drug-like properties and good ADMET properties within the required allotted limitations. The data obtained in the current work highlighted the potential application of groundnut cakes for the eco-friendly and scaled-up production of HPC, a new anti-α-glucosidase agent that should be further investigated for type 2 diabetes management.

Keywords: diabetes; α-glucosidase inhibitors; hemi-pyocyanin; organic industrial waste; peanut oil processing by-product; fermentation; bioreactor systems

1. Introduction

Agricultural production releases a significant amount of organic waste. Untreated waste may cause serious pollution for the environment, which is becoming a threat to global health and food security [1]. However, agricultural waste (AW) is rich in essential nutrients, such as proteins, lipids, glucid, and minerals, and as such, AW may be used for many purposes [2,3]. Recently, recycling AW for the bioproduction of valuable secondary metabolites via bacterial conversion has become an emerging topic [1,4]. In this work, a peanut oil processing by-product (named groundnut cake, GNC) was investigated for the bioproduction of bioactive hemi-pyocyanin (HPC) via microbial conversion.

The peanut belongs to the family *Fabaceae*, commonly known as the legume family, and is native to Central and South America [5]. Up to now, this crop has been widely planted in Asian countries and Asia was ranked first in the world for total area under peanut plantations, with Vietnam ranked 15th with 456,513 tons [6]. Peanut seeds are rich in oil; as such, it is considered a major oil crop and is ranked fourth among oil-producing seeds worldwide [7]. During peanut seed processing for peanut oil, approximately 50%

of the generated material is the by-product groundnut cake (GNC) [8]. GNC is widely used for feeding animals or as fertilizer [9]. Recently, GNC has also been used as an N/C source for microbial fermentation to produce bioactive secondary metabolites [10–12]. In the current work, we studied the use of GNC for the bioproduction of an α-glucosidase inhibitor compound targeting anti-diabetic drugs.

Diabetes mellitus is a major health issue that has significant negative effects on the quality of life and health of people worldwide [13]. The two major types of diabetes mellitus include type 1 and type 2 diabetes (T2D). Of these, T2D accounts for 90% of diabetes cases [14]. Among the several modes of T2D management, α-glucosidase inhibitors (aGIs) are considered effective [15,16]. To date, some commercial aGIs (acarbose, voglibose, and miglitol) have been synthesized and are available for use; however, these inhibitors have been reported to show various side effects and as such, the search for novel aGIs from natural sources continues [17]. aGIs are isolated from several natural sources, particularly medicinal plants [16,18,19]. However, it is quite difficult to acquire a large amount of aGIs from medicinal herbs [20–22]. Microbial fermentation is a robust tool for producing high yields of various bioactive secondary metabolites, including aGIs [20,23–25]. In this work, we reported the scaled-up production of the aGI hemipyocyanin (HPC) via microbial fermentation.

Phenazine is a heterocyclic nitrogenous compound with the formula $(C_6H_4)_2N_2$. From the basic structure of phenazine, various derivatives of phenazine compounds have been created and more than 100 natural phenazines from microbes have been investigated [26,27]. *Pseudomonas* species produce more than 50 phenazine compounds [28,29]. Of these, *Pseudomonas aeruginosa* is a major phenazine-producing strain; however, almost all previous works have used commercial media for the biosynthesis of phenazine compounds and fermentation has been performed on a small scale in flasks. In addition, pyocyanin, a major phenazine compound, has been extensively investigated, while there are only a few reports on HPC production by *P. aeruginosa* and its biological effects [30–32].

In our previous work [33], HPC was investigated as the main secondary metabolite produced by TUN03 strain fermentation. In this study, we explored the potential use of organic waste for the eco-friendly production of HPC via *P. aeruginosa* TUN03 fermentation. This active compound was further studied for scaled-up production utilizing a bioreactor system. The α-glucosidase inhibitory effect of HPC was also investigated via in vitro assays and virtual performance.

2. Results and Discussion

2.1. Determination of the Mineral Salt Content of the Peanut Oil Processing By-Product GNC

Some of the essential nutrient contents, such as proteins, lipids, glucid, and minerals, in the starting material (GNC) were determined and the results are presented in Table 1. The results indicated that the GNC was rich in protein (35.04%) and lipids (9.66%), while a small amount of total sugar (2.51%) and reducing sugar (0.612%) was found in this substrate. The total mineral content of the GNC was 12.52%. To elucidate the composition of mineral elements, we used SEM capture for the analysis of GNC ash. The data (Figure 1) showed that there were diverse elements (O, C, Al, Fe, Si, and K) contained in the GNC ash. Of these, Al, Fe, Si, and K were the main mineral elements of the GNC ash. These elements have been evidenced as having important roles in the growth of bacteria [12]. The results obtained in this work were similar to those in some previous reports, indicating that GNC is rich in protein, lipids, and minerals, as well as some other components [9,10,34]. These data indicated that GNC would be a suitable substrate for bacterial fermentation to produce secondary metabolites.

Table 1. The determination of the nutrient contents contained in the GNC.

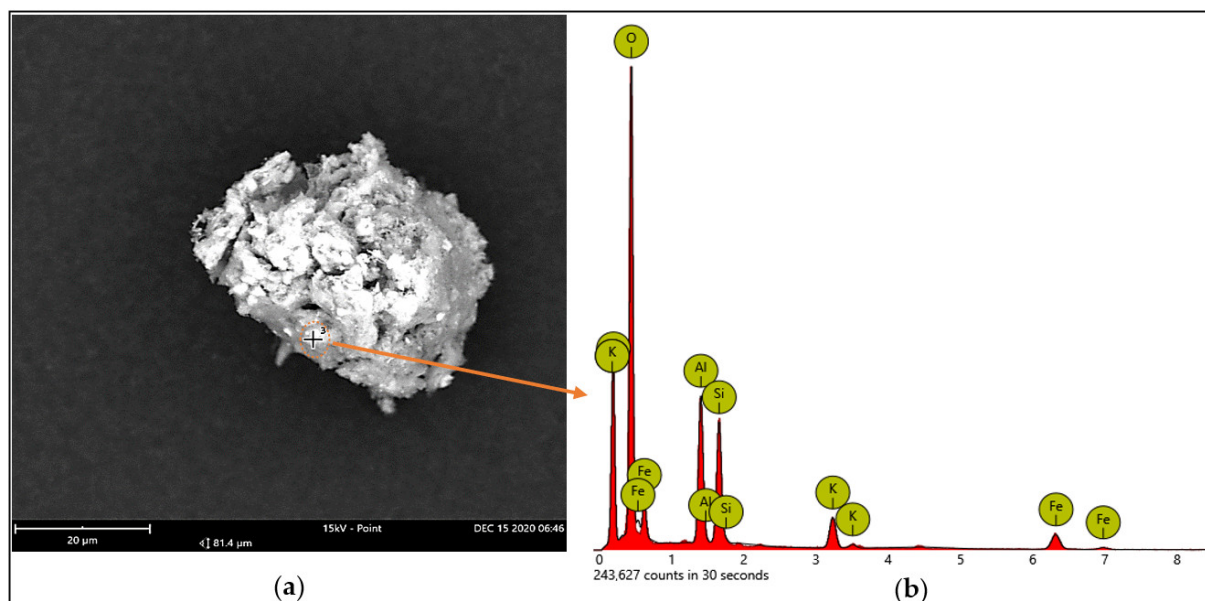| Proteins	Lipids	Total Sugar	Reducing Sugar	Total Minerals
35.04%	9.66%	2.51%	0.612%	12.52%

Figure 1. The analysis of the mineral elements of the GNC ash using SEM capture: the SEM image of the analyzed point on the surface of the GNC ash (**a**); the mineral elements of the GNC ash, as detected by EDX spectra (**b**).

2.2. Production of Hemi-Pyocyanin via P. aeruginosa TUN03 Conversion

Several significant factors affecting HPC yield were examined to establish the process of culturing TUN03 bacteria to produce high yields of hemi-pyocyanin (HPC). We examined the effects of C/N sources (1), salt composition (2), and scaled-up HPC production in a bioreactor system (3).

(1) Effects of C/N sources on hemi-pyocyanin bioproduction. Various C/N sources, including the peanut oil processing by-product groundnut cake (GNC) and some commercial culture broths, including tryptic soy broth (TSB), nutrient broth (NB), and King's B (KB), were used for fermentation. For comparison, soybean waste (SBW) and squid pen waste (SPW) were also used for fermentation by *P. aeruginosa* TUN03 over 6 days and then the HPC contents in the fermented culture broths were determined. The data in Figure 2a show that the highest production of HPC was found on day 3 of fermentation. The HPC yield was moderate (in the range of 8–13 μg/mL) in the culture broths containing commercial media (NB, TSB, and KB), while HPC was found to be produced at a higher yield (13.1–18 μg/mL) in the culture broths containing organic processing by-products (GNC, SBW, and SPW). Of these, GNC was the best C/N source for bacterial cultivation with the highest HPC yield of 18 μg/mL. Thus, this low-cost material was chosen for further experiments. Various culture broths containing different concentrations of GNC (0.5–2.0%) were used for fermentation and then the HPC contents were determined on day 3 of cultivation. The experimental data (Figure 2b) indicated that high yields of HPC were produced when the concentration of GNC was from 1.25% to 1.75%. Thus, for the cost-effective bioproduction of HPC, 1.25% GNC was used in the subsequent bacterial cultivation experiments.

(2) Effects of salt composition on HPC bioproduction. The bacterial culture media were supplemented with some sulfate and phosphate salt sources to assess their effects on HPC bioproduction. Among the tested sulfate salts, $MgSO_4$ significantly enhanced HPC production (19.5 μg/mL; Figure 2c) via *P. aeruginosa* TUN03 and the most suitable concentration was found to be 0.075% (Figure 2d). K_2HPO_4 was found to be the most suitable kind of phosphate salt (Figure 2e) and its most suitable concentration was recorded to be 0.075% (Figure 2f).
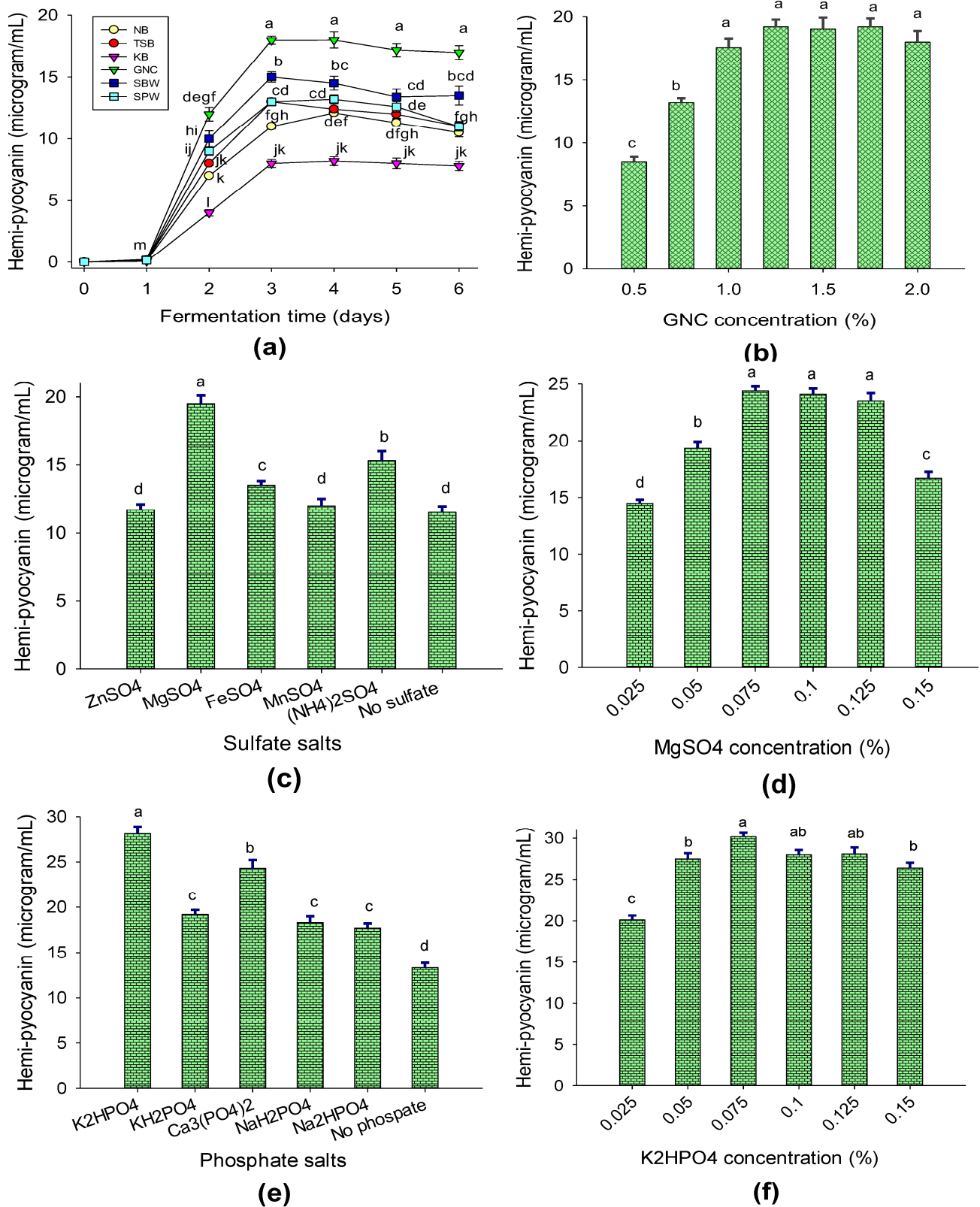
Figure 2. The effects of C/N source (**a**), GNC concentration (**b**), sulfate salt source (**c**), MgSO$_4$ concentration (**d**), phosphate salt source (**e**), and K$_2$HPO$_4$ concentration (**f**) on HPC production via *P. aeruginosa* TUN03. The tests were conducted in triplicate. HPC yield values in the same figure with the same letters were considered as not significantly different via Duncan's multiple range test (*p* = 0.05).

(3) Effects of selected culture parameters on HPC biosynthesis.

To reach higher HPC production via TUN03 strain conversion, selected culture conditions, such as the temperature of cultivation (25, 27.5, 30, 32.5, and 35 °C), the culture medium pH (pH 6.0, 6.5, 6.0, 7.5, 8.0, 8.5, and 9.0), and the time course of cultivation (0, 1, 2, 3, and 4 days), were examined. Taken together, *P. aeruginosa* TUN03 was found to produce the highest HPC content when it was fermented under the conditions of a cultivation temperature of 30–32.5 °C (Figure 3a), an initial pH of 6.5–7.0 (Figure 3b), and a fermentation time of 2–3 days (Figure 3c). The density of bacteria was also examined during the fermentation; however, no correlations between HPC yield and bacterial culture density (the data are not shown) were observed.
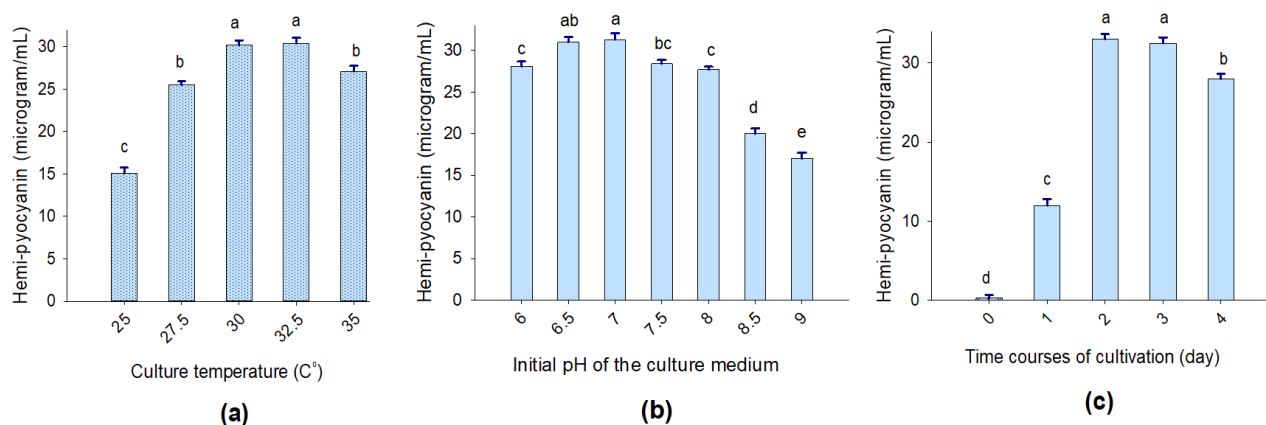

Figure 3. The effects of culture temperature (**a**), the initial pH of the culture medium (**b**), and fermentation time (**c**) on HPC production via *P. aeruginosa* TUN03 fermentation. The tests were conducted in triplicate. HPC yield values in the same figure with the same letters were considered as not significantly different via Duncan's multiple range test at $p = 0.05$ (**b**) and Fisher's LSD test at $p = 0.05$ (**a**,**c**).

(4) Scaled-up HPC production using a 14 L bioreactor system.

In fermentation technology, bioreactor systems are valuable pieces of equipment that can effectively produce high yields of secondary metabolites with quick fermentation processes [35]. In this study, a 14 L bioreactor system was utilized for scaled-up HPC production. As shown in Figure 4, HPC was biosynthesized after 4 h and the maximal productivity was produced after 8 h of fermentation. Thus, HPC was biosynthesized with higher yields (35.1 µg/mL) in a much shorter fermentation period (8 h) than when it was biosynthesized on a small scale in flasks, which had a lower productivity of 30.2 µg/mL and a longer cultivation time (3 days).

Phenazine compounds possess numerous valuable bioactivities and applications and thus, their production has received much attention. In most previous studies, phenazines have been produced by *P. aeruginosa*, utilizing commercial broths as the main C/N sources, including King's B, King's A, peptone, tryptone, and nutrient broth, for fermentation. Phenazines have been produced with productivity values in the range of 5.2–33 µg/mL [36–40]. To lower the costs of the bioproduction of phenazines, several low-cost organic materials, such as cottonseed, corn, grape seed, taro leaves, peat moss, sweet potato, soya bean, groundnut, and watermelon seeds, have been used for fermentation; however, these produced low yields of phenazines (under 4.0 µg/mL) [39,41,42]. For cost-effective and eco-friendly production, several organic by-products/waste materials have been used for fermentation, such as waste cheese whey, tea wastewater, waste frying oil, maize wastewater, olive waste, sugar beet molasses, peapods, and craft beer waste, which produced phenazine yields of 1.62, 2.0, 3.0, 3.2, 1.3, 1.6, 17.1, and 21–58 µg/mL, respectively [41,43–46]. In our current report, GNC was used as the main C/N source for the biosynthesis of HPC, resulting in the high-level productivity of 35.1 µg/mL. In addition, in almost all previous works, phenazine produc-

tion has been conducted on a small scale in flasks over long fermentation times. Different from those, in our study, the phenazine compound was mass-biosynthesized utilizing a 14 L reactor over a shortened cultivation period (12 h). The results recorded in this work demonstrate the new and green utilization of GNC for the eco-friendly production of HPC.
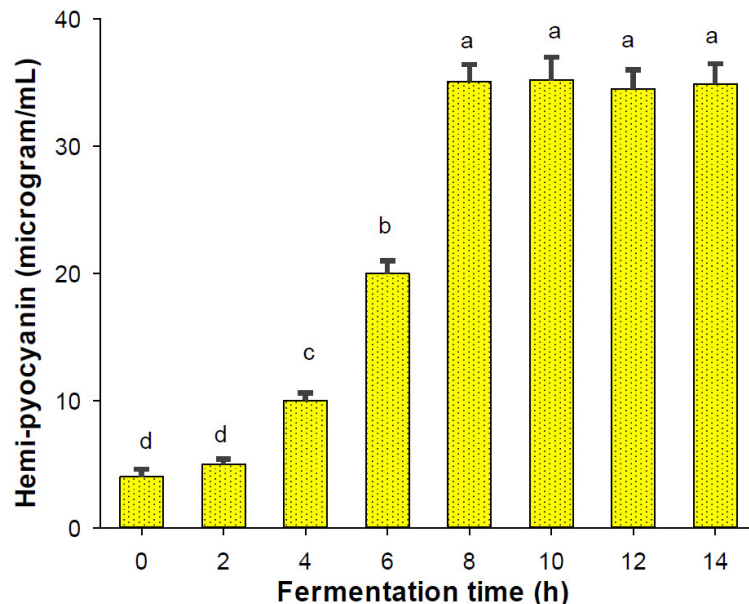

Figure 4. The scaled-up production of HPC using a 14 L bioreactor system. The tests were conducted in triplicate. HPC yield values in the same figure with the same letters were considered as not significantly different via Duncan's multiple range test ($p = 0.05$).

2.3. Purification and Identification of Hemi-Pyocyanin

The yellow compound was purified according to the method presented in our earlier report [33] and this purification protocol is summarized in Figure 5.
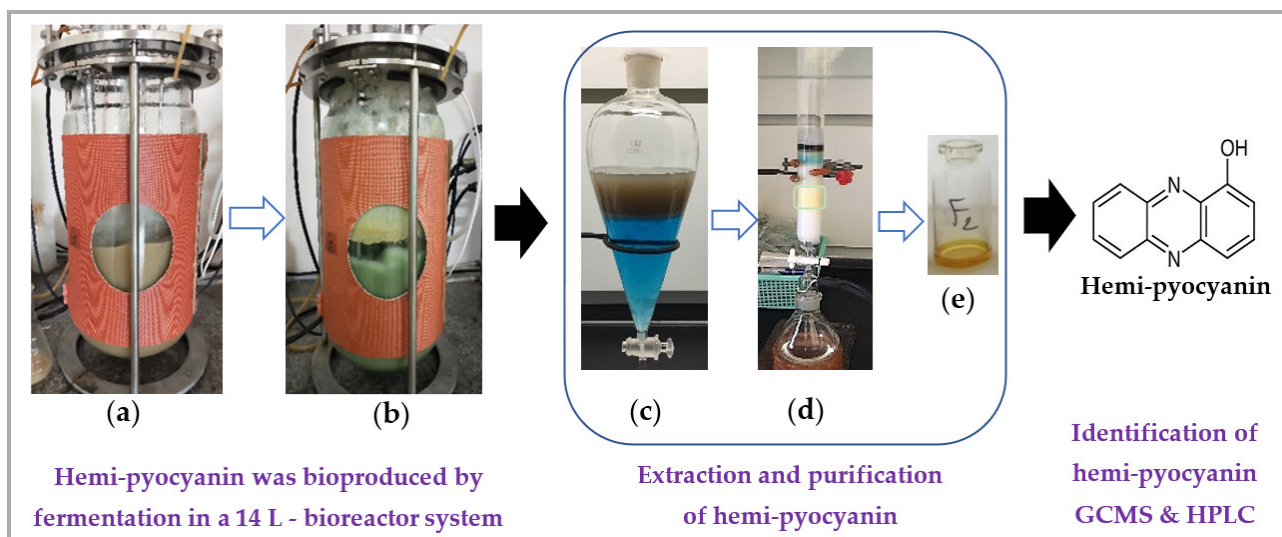
Figure 5. The process of the bioproduction, purification, and identification of hemi-pyocyanin (HPC). The liquid culture medium (5 L) containing 1.25% GNC (**a**) was fermented by the TUN03 strain in a reactor for 8 h (**b**). The pigment (HPC) was purified by a liquid layer of chloroform (**c**) and was then isolated using a column loaded with silica gel (**d**) to obtain the pure compound in yellow form (**e**), which was identified as HPC by GCMS. The pure grade of the HPC was then checked by HPLC analysis.

The compound purified from the medium fermented by the TUN03 strain was reconfirmed as HPC and its purity grade was also determined by HPLC and GCMS analysis. As shown by the data presented in Figure 6, the purified HPC appeared with a single peak at the retention time of 3.317 min. For comparison purposes, the reference HPC compound obtained in our previous report [33] also underwent HPLC analysis. This reference compound also appeared at the retention time of 3.323 min during HPLC fingerprinting (Figure 6), approximately similar to that of the HPC purified in this study (RT = 3.317 min). The HPC had 100% of the relative area, thus indicating that the HPC produced and purified in this report had a high grade of purity and could be used for bioactivity testing. GCMS was also conducted for identification. The GCMS data indicated that the compound purified in this study was HPC (Figure A1 in Appendix A). For a more careful confirmation, the ^{1}H-NMR and ^{13}C-NMR spectra of the HPC were also analyzed. The HPC compound was obtained as a yellow amorphous powder with ^{1}H-NMR (600 MHz; CDCl$_3$) (δH = 8.38 (1H, m); δH = 8.279–8.366 (2H, m); δH = 7.826–7.919 (4H, m); δH = 7.260–7.289 (1H, m)) (Figure A2a in Appendix A) and ^{13}C-NMR (151 MHz; CDCl$_3$) (δC = 151.69; 144.30; 144.50; 141.19; 134.70; 131.89; 130.80; 130.50; 129.68; 129.18; 119.90; 108.89) (Figure A2b in Appendix A). These assigned ^{1}H-NMR and ^{13}C-NMR data were approximately similar to those of the compound reported in our earlier study [33].
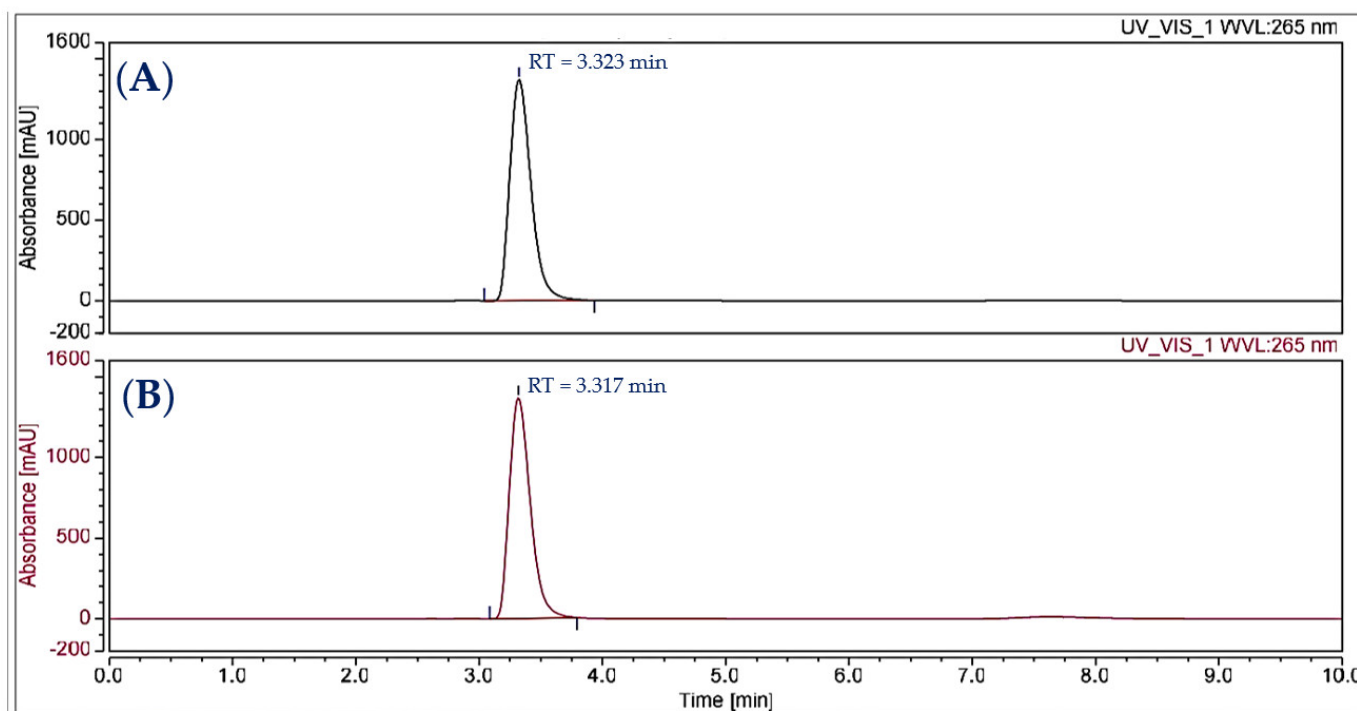
Figure 6. The HPLC analysis of the reference compound (**A**) and the yellow HPC purified in this study (**B**).

2.4. The α-Glucosidase Inhibitory Effects of Hemi-Pyocyanin: In Vitro Experiments and Docking Studies

Diabetes mellitus has significant negative effects on the quality of life and health of people worldwide [13]. Of the two major types of this disease, type 2 diabetes (T2D) accounts for up to 90% of diabetes cases [14]. To date, there are several therapies for the treatment of T2D; of these, the use of inhibitors for α-glucosidase and α-amylase is considered an effective treatment for T2D [15,16]. In our previous work [33], the anti-α-amylase effect of HPC was recorded for the first time. In this work, we investigated the potential anti-α-glucosidase effects of this microbial secondary metabolite via in vitro and docking studies.

2.4.1. The Assessment of α-Glucosidase Inhibitory Effects

The crude extract, crude pigments (chloroform layer), purified HPC compound, and acarbose (a commercial α-glucosidase inhibitor compound) were tested at various concentrations to investigate their effects against the α-glucosidase enzyme from yeast. As shown in Figure 7a, the crude extract showed a moderate anti-α-glucosidase effect with a maximum inhibition value of 82% at a high concentration (5 mg/mL). The crude pigments demonstrated a high effect with an inhibition value of 100% at a concentration of 2.5 mg/mL. The purified HPC compound showed the highest effect with a maximum inhibitory effect (approximately 100%) at the low concentration of 1.25 mg/mL. This result indicated that the activity significantly increased after purification and that the purified HPC compound was a major α-glucosidase inhibitor when produced by *P. aeruginosa* TUN03. Acarbose, a commercial α-glucosidase inhibitor, was also assessed for comparison and showed a maximum inhibition value of 85% at 2.5 mg/mL.
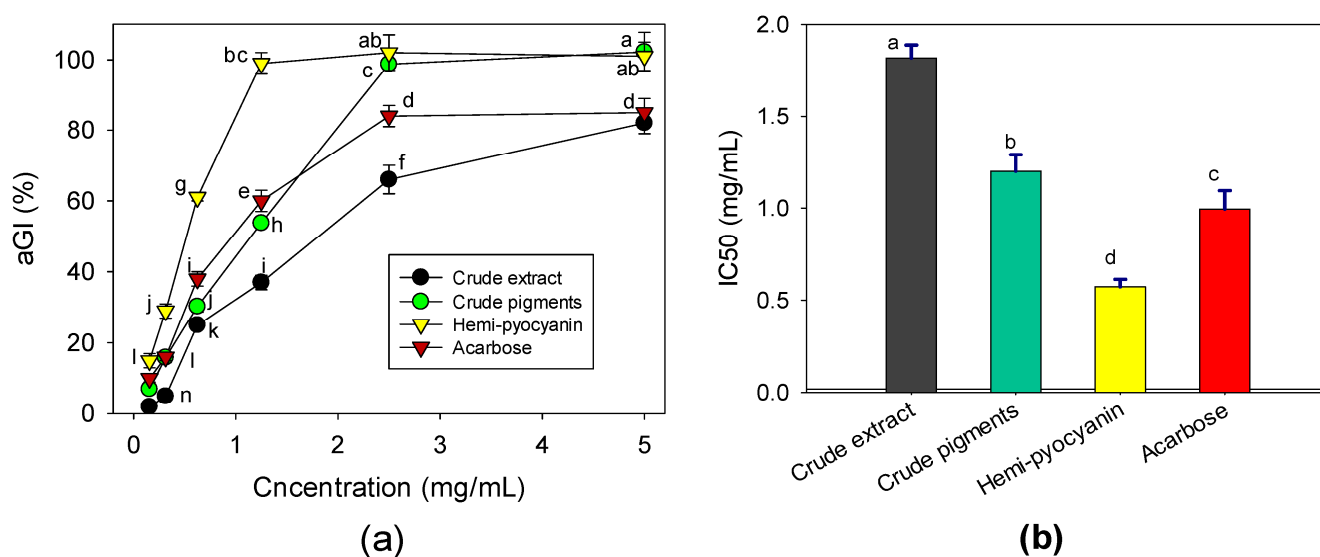

Figure 7. The anti-α-glucosidase effects of the crude extract, crude pigments, hemi-pyocyanin, and acarbose. The effects are expressed as the inhibition value % (**a**) and IC50 value (**b**). The tests were conducted in triplicate. HPC yield values in the same figure with the same letters were considered as not significantly different via Fisher's LSD test at $p = 0.05$.

For a further clarification of the results, the inhibitory effects were also expressed as IC50 values, defined as the concentration of an inhibitor that inhibits 50% of enzymatic activity. Therefore, the lower the IC50 value that an inhibitor shows, the greater the inhibition it achieves [19]. Based on the IC50 values (Figure 7b), the crude extract demonstrated the lowest activity since it possessed the highest IC50value (1.82 mg/mL). The crude pigments showed comparable activity to acarbose with IC50 values of 0.994 and 1.19 mg/mL, respectively. Meanwhile, the HPC inhibited α-glucosidase with a low IC50 value (0.572 mg/mL); therefore, it had a higher effect than acarbose. This experimental data confirmed that HPC is a potential α-glucosidase inhibitor. Notably, the novel and potential anti-α-glucosidase effect of HPC is presented for the first time in our current report.

Postprandial hyperglycemia is an important effect of T2D development; thus, to delay or prevent T2D, it is necessary to control blood glucose [47]. The inhibitory effect of a-amylase and a-glucosidase, the glycosidases that convert dietary starch into glucose, has been widely used to control plasma glucose [15,48] and this therapy has been found to be a more effective method than controlling insulin secretion due to its economic benefits, convenience, and minimization of negative effects [49]. The basic biochemical process of using glycosidase inhibitors may be briefly summarized as follows. The enzyme α-amylase catalyzes a-(1,4)-glycosidic linkages in starch to release mainly disaccharide (maltose),

which is finally hydrolyzed into monosaccharide (glucose) via the action of α-glucosidase before entering blood circulation via intestinal epithelial absorption [49]. Notably, HPC has demonstrated a potent effect against both α-amylase [33] and α-glucosidase (a novel finding in this study) and thus, HPC may be a potent microbial compound for the treatment of T2D and obesity.

Among the phenazine compounds biosynthesized by *P. aeruginosa*, numerous studies have reported the bioproduction of pyocyanin and its various bioactivities; however, there have only been a few reports on the production and bioactivities of HPC [31,50–55]. To date, HPC has been reported to have some bio-effects, such as anti-cancer [51,52], anti-microbial [31,51–54], and anti-inflammatory effects [55]. Thus, the novel α-glucosidase inhibitory activity of HPC reported in this work may enrich the catalog of the biological activities of HPC.

2.4.2. The α-Glucosidase Inhibitory Effect via Docking Simulations

Docking simulations were performed to understand the energy binding and interaction of the inhibitors with the target enzyme. α-Glucosidase structure data were downloaded from Worldwide Protein Data Bank and then their 3D structures were prepared using MOE-2015.10 software. The active sites (ASs) of ligands on α-glucosidase were found using a site finder and the five most active sites (AS1, AS2, AS3, AS4, and AS5) were determined (Figure A3). Both ligands effectively bound to the target enzyme at AS1; thus, this active site was chosen for assessing the docking simulation performance.

In the virtual performance, root mean square deviation (RMSD) and docking score (DS) were used as indicators for the determination of the successful interactions between the inhibitors and the enzyme and its effective inhibition, respectively. The interactions between the ligands and the enzyme were considered as significant and acceptable when the RMSD value was less than 2.0 Å [56]. A compound was determined to be an effective enzyme inhibitor when the DS value was less than -3.20 kcal/mol [57]. As summarized in Table 2, the HPC and ACA ligands bound to the enzyme with RMSD values of 1.298 and 1.496 Å, respectively, which were lower than 2.0 Å; thus, the interactions between these ligands and the enzyme were significant and accepted [56]. In addition, both of these ligands interacted with the target enzyme to generate the very low DS values of -9.0 and -10.1 kcal/mol, respectively; thus, both HPC and acarbose were confirmed as effective and potential α-glucosidase inhibitors via our docking simulations. The docking simulation results (Table 2) and in vitro assays (Figure 7) were in agreement.

Table 2. The docking study results for the interactions between the inhibitors and the target protein α-glucosidase (aG).

Ligand	Symbol	RMSD (Å)	DS (kcal/mol)	Bonds	Amino Acids Interacting with the Ligands (Distance(Å)/E(kcal/mol)/Linkage Type)
Hemi-pyocyanin	HPC-aG	1.298	-9.0	3 bonds (1 H-acceptor, 2 pi-H)	Lys156 (3.21/-3.2/H-acceptor) Leu313 (4.08/-0.6/pi-H) Arg315 (4.22/-0.6/pi-H)
Acarbose	ACA-aG	1.496	-10.1	9 bonds (6 H-donor, 2 H-acceptor, 1 H-pi)	Glu411 (2.65/-3.2/H-donor) Tyr158 (2.96/-2.3/H-donor) Pro312 (2.65/-3.2/H-donor) Asp352 (2.79/-2.2/H-donor) Glu277 (2.78/-3.8/H-donor) Asp242 (3.21/-1.0/H-donor) Arg442 (3.30/-0.9/H-acceptor) Lys156 (3.01/-1.0/H-acceptor) Tyr158 (3.36/-0.7/H-pi)

To explore the interactions between the ligands and the target protein, simultaneous interactions and bonds were examined in detail, as illustrated in Figures 8 and 9. As shown in Figure 8, HPC bound to the enzyme at the AC1 site via interactions with some prominent amino acids at the biding sites, including Lys156, Leu313, and Arg315, and generated three bonds: one H-acceptor bond and two pi-H bonds. Of these, the H-acceptor bond was formed by the connection of the N2 atom of the HPC ligand to the NZ of Lys156, with a distance of 3.21 Å and an energy binding of 3.2 kcal/mol, while the six rings of the HPC ligand were found to be connected to the CA and N of the amino acids Leu313 and Arg315. The two pi-H bonds were formed with the distance and energy binding values of 4.08 Å and 4.22 Å and −0.6 kcal/mol and −0.6 kcal/mol, respectively. The commercial inhibitor, acarbose bound effectively to α-glucosidase at active site 1 by creating nine bonds, including six H-donor bonds, two H-acceptor bonds, and one H-pi bond (Figure 9). The detailed distance and energy binding values of these bonds were also recorded and are summarized in Table 2. Based on the results of the in vitro studies and docking investigation, the HPC compound produced in this work could be recommended as a good candidate as a potential α-glucosidase inhibitor, which may be useful for T2D management. However, further studies should be conducted in animal models, as well as clinical investigations, for the development of HPC into a drug with antidiabetic and anti-obesity functions.
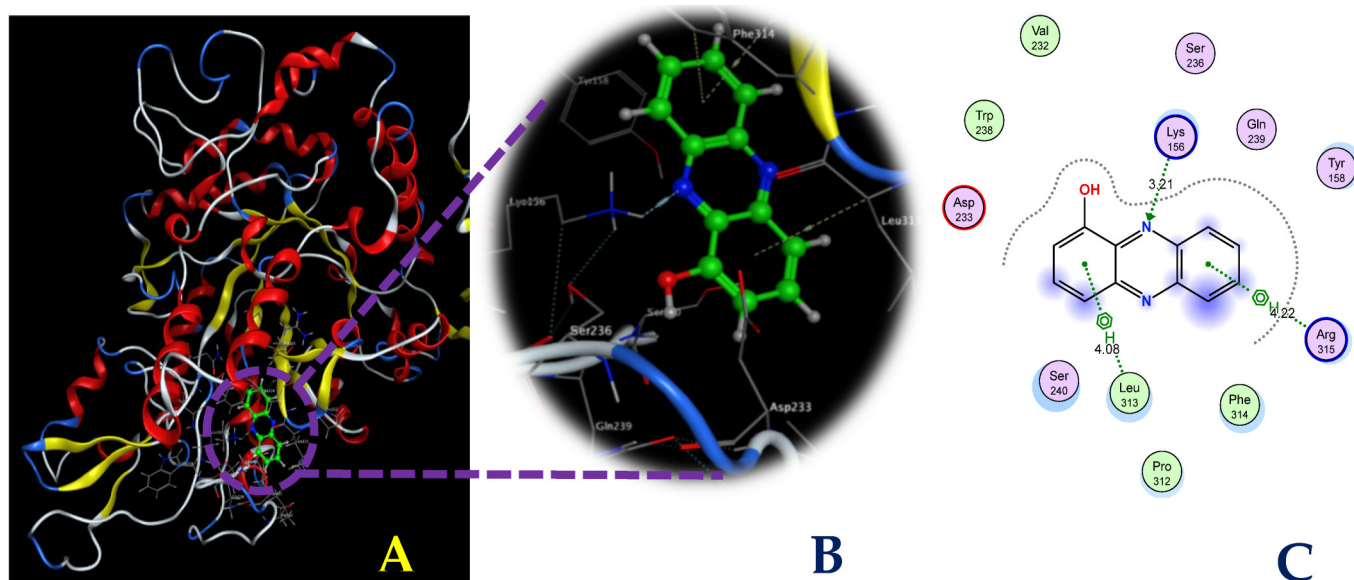

Figure 8. The interaction between hemi-pyocyanin and the enzyme α-glucosidase (**A**) and the 3D (**B**) and 2D (**C**) structures of the hemi-pyocyanin ligand at active site 1 of α-glucosidase.

2.5. Lipkin's Rules and ADMET-Based Pharmacokinetics and Pharmacology

Five Lipkin's rules are commonly used to explore whether an active compound possesses drug-like properties, such as a molecular mass less than 500 Da (rule 1), high lipophilicity with a LogP value < 5 (rule 2), H-donors < 5 (rule 3), H-acceptors < 10 (rule 4), and molar refractivity between 40–130 (rule 5). The probability of success for drug-like compounds can be predicted when they possess more than two Lipkin's rules [58]. As shown in Table 3, hemi-pyocyanin complied with all five Lipkin's rules; as such, this inhibitor has a high probability of being successfully developed as a drug. Acarbose, a commercial α-glucosidase inhibitor, was also examined against these rules; however, this compound only satisfied approximately two rules. The ADMET properties of hemi-pyocyanin and acarbose were also studied and the data are presented in Table A1 in Appendix A. In general, these tested inhibitor compounds also had good ADMET properties in the required allotted limitations.
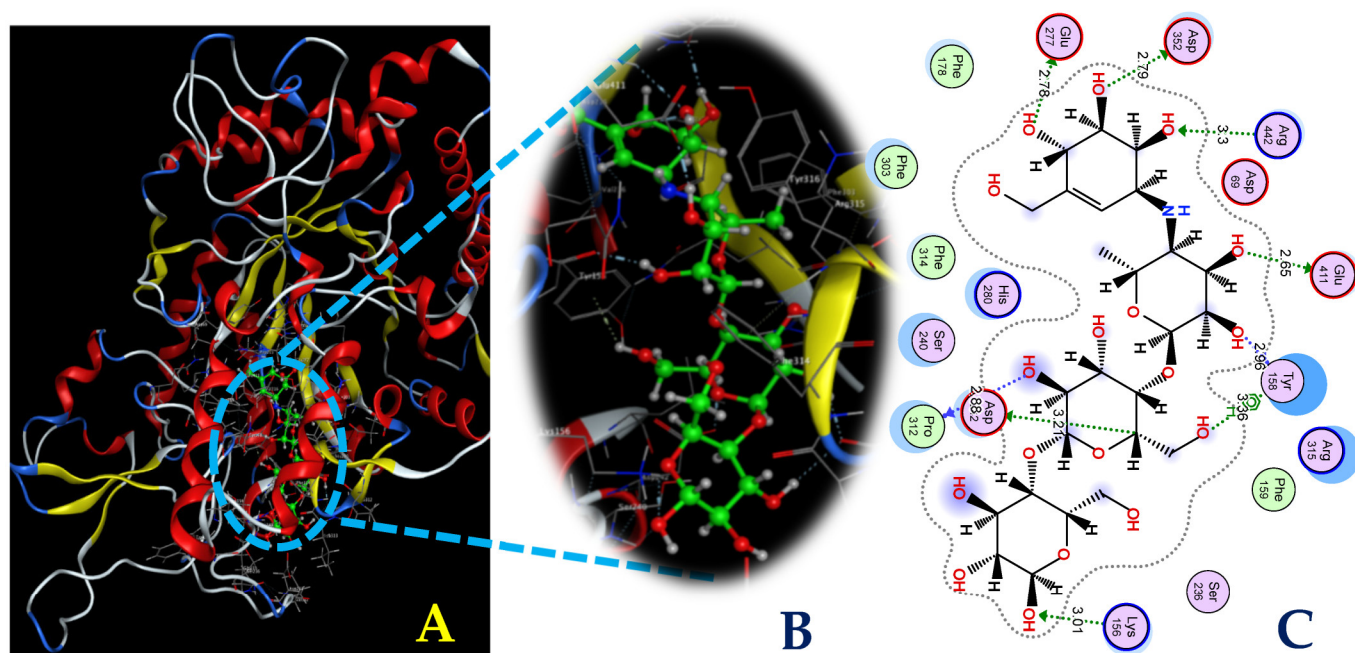
Figure 9. The interaction between acarbose and the enzyme α-glucosidase (**A**) and the 3D (**B**) and 2D (**C**) structures of the acarbose ligand at active site 1 of α-glucosidase.

Table 3. The results of the five Lipkin's rules for hemi-pyocyanin and acarbose.

Compound	Mass (Dalton)	H-Donor	H-Acceptors	LogP	Molar Refractivity
Hemi-pyocyanin	196.0	1	3	2.49	58.7
Acarbose	646.0	15	19	−9.6	136.5
Lipkin's rules	≤500	≤5	≤10	≤5	40–130

3. Materials and Methods

3.1. Materials

The *P. aeruginosa* TUN03 strain used for fermentation in this report was acquired from our earlier study [33]. The α-glucosidase originated from *S. cerevisiae* and the commercial anti-α-glucosidase compound (acarbose) was acquired from Sigma Chemical Co., St. Louis City, MO, USA. The substrate (p-nitrophenyl glucopyranoside, pNPG) was purchased from Sigma Aldrich (3050 Spruce Street, St. Louis, MO, USA). The silica gel (Geduran® Si 60, size 0.040–0.063 mm) was commercially obtained from Merck Sigma Chemical Co. (St. Louis City, MO, USA) and some solvents were obtained from Sigma Aldrich.

3.2. Methods

3.2.1. Production of Hemi-Pyocyanin via Microbial Fermentation Experiments

- Protocols for determining the nutrient contents of GNC. The essential nutrient ingredients contained in the GNC were examined. The protein content [59], total mineral content of the ash [59], mineral composition (using a generation 5 phenom pro and proX SEMs), total lipid content [60], total dissolved sugar content [61], and reducing sugar content [62] were determined.

- The effects of C/N source on hemi-pyocyanin produced by the TUN03 strain. Six kinds of materials, including NB, TSB, KB, GNC, soybean waste, and squid pen waste, were used as sole C/N sources for fermentation by the TUN03 strain. A liquid medium (30 mL in a 100 mL flask) containing 1% C/N source, 0.05% $MgSO_4$ salt, and 0.1% $Ca_3(PO_4)_2$ salt with an initial pH of 7 was fermented by the TUN03 strain at 30 °C with a shaking speed of 150 rpm for 6 days (*). The supernatant was collected daily by centrifuging at a rotation speed of $10,000 \times g$ for 10 min. The collected supernatant was then used for the determination of the HPC yields produced by the TUN03 strain. GNC was chosen for all further experiments. To determine the optimal concentration of GNC, different concentrations (0.5%, 0.75%, 1.0%, 1.25%, 1.5%, 1.75%, and 2.0%) were added into a medium containing 0.05% $MgSO_4$ salt and 0.1% $Ca_3(PO_4)_2$ salt with an initial pH of 7, which was then fermented by *P. aeruginosa* TUN03 using above protocol (*) over 3 days. Then, the supernatant was harvested and used to detect the HPC content.

- The effects of salt composition on hemi-pyocyanin produced by the TUN03 strain.

  - † The effect of sulfate salts on hemi-pyocyanin bioproduction. Five sources of sulfate salts, including $ZnSO_4$, $FeSO_4$, $(NH_4)_2SO_4$, $MnSO_4$, and $MgSO_4$, were tested for their effects. A culture broth containing 1.25% GNC, 0.05% sulfate salt, and 0.1% $Ca_3(PO_4)_2$, with an initial pH of 7 was cultivated by the TUN03 strain using the above protocol (*). The supernatant obtained after 3 days of cultivation was used for the determination of the HPC content. $MgSO_4$ was found to be the most suitable for enhancing HPC yield; thus, this salt was added into the culture broth at different concentrations (0, 0.025, 0.05, 0.075, 0.1, 0.125, and 0.15) to check its effect on HPC production and 0.075% was found to be the most suitable concentration. Thus, 0.075% $MgSO_4$ was used for further investigation.

  - † The effect of phosphate salts on hemi-pyocyanin bioproduction. Five sources of phosphate salts, including KH_2PO_4, NaH_2PO_4, $Ca_3(PO_4)_2$, K_2HPO_4, and Na_2HPO_4, were tested. A culture broth containing 1.25% GNC, 0.075% $MgSO_4$, and 0.1% phosphate salt with an initial pH of 7 was fermented by the TUN03 strain using the above protocol (*) over 3 days. The supernatant was collected and used for the detection of the HPC content. K_2HPO_4 was found to be the most suitable for enhancing HPC yield; thus, this salt was added into the medium at different concentrations (0, 0.025, 0.05, 0.075, 0.1, 0.125, and 0.15) to check its effect on HPC production and the most suitable concentration was 0.075%. Thus, this concentration was used for further investigation.

- Mass-production of hemi-pyocyanin via P. aeruginosa TUN03 fermentation in a bioreactor. HPC bioproduction was scaled up using a 14 L bioreactor system. *P. aeruginosa* TUN03 was pre-incubated in a nutrient broth using 500 mL flasks at 30 °C for 1.5 days. Then, 600 mL of bacterial seed was added to the reactor, which contained 5.4 L of a newly designed culture broth containing 1.25% GNC, 0.075% $MgSO_4$, and 0.0.075% K_2HPO_4 with an initial pH of 7. The cultivation was performed at 30 °C (culture temperature), 250 rpm (shaking speed), and 1.2 vvm (dissolved oxygen content) for 14 h. The HPC yield was determined every 2 h.

3.2.2. Quantitation, Purification, and Identification of Hemi-Pyocyanin

Quantitation of HPC via HPLC analysis. The residues of the culture medium and *P. aeruginosa* TUN03 biomass were removed by centrifuging at 8000 rpm for 10 min. Then, the supernatant was collected and used to determine the HPC content via HPLC analysis. Then, 5 µL of supernatant was injected into the HPLC system for analysis. A column (C18) was used to separate the sample with the use of solvent systems, including methanol and acidified 0.1% H_3PO_4 at a ratio of 70/30 (*v/v*). The flow rate (0.2 mL/min) was set and the HPC compound was detected at a wavelength of 265 nm. A reference HPC

compound purified in our earlier report was tested to establish the following equation for the stimulation of HPC content:

$$\text{HPC content: } y = 0.3954x + 0.1583$$

where the area value of the HPC peak and the concentration of HPC were named y and x, respectively. All tests were performed in triplicate.

Purification and identification of HPC. The method presented by Nguyen et al. [33] was applied for the extraction and isolation of the yellow pigment. A culture broth fermented by the TUN03 strain was centrifuged at 12000 rpm for 10 min for the residues of the culture medium and *P. aeruginosa* TUN03 biomass to settle down. The supernatant (250 mL) was collected and mixed with chloroform (250 mL). This mixture was slightly mixed and kept in a glass funnel (1000 mL) for approximately 3 h. The chloroform layer was concentrated using an evaporator (IKA, Staufen, Germany) at 55 °C under a vacuum. The sample was further dried to form a powder (crude pigments) at a temperature of 55 °C in an air-drying oven. Finally, the sample was separated via a column (30 × 2 cm) containing silica (size 0.040–0.063 mm; Geduran® Si 60) and chloroform to collect the yellow compound. This pigment compound was later identified as HPC via GCMS and HPLC analysis [33].

3.2.3. Bioactivity Assays

The anti-α-glucosidase activity assay. The anti-α-glucosidase effect was examined according to the protocol described in our previous work [23]. DMSO was used for the preparation of the crude extract, crude pigments, purified compound (HPC), and acarbose solution. A buffer of potassium phosphate (0.1 mol/L; pH 7) was applied for the preparation of the α-glucosidase and *p*-NPG solution. The experiments were performed in 96-well templates and the protocol followed three typical steps, as follows:

① Preincubation. Firstly, 100 μL of the α-glucosidase solution and 50 μL of a sample solution were loaded into a 96-well template. This solution was pre-incubated at a temperature of 37 °C for 20 min.

② Reaction period. To start this step, 50 μL of 10 mmol/L *p*-NPG solution was loaded into a well and maintained at 37 °C for 30 min. Finally, the reaction was terminated after adding 100 μL of 1 mol/L Na_2CO_3.

③ Measurement of absorbance and bioactivity calculation. The absorbance of the solution obtained in step 2 was measured at a wavelength of 410 nm (namely Ex). A control test was carried out as described in the above two steps but 50 μL of 0.1 mol/L potassium phosphate buffer (pH 7) was used instead of the sample solution. The absorbance was also measured at 410 nm (namely Co). The aGI (%) was estimated according to the following equation:

$$\text{aGI (\%)} = (\text{Co} - \text{Ex})/\text{Co} \times 100.$$

The IC50 value is defined as the concentration of an inhibitor that inhibits 50% of the enzymatic effect [63].

3.2.4. The Docking Study Protocol

The virtual study was performed according to the protocol presented in our earlier work [64] and followed three typical steps, as follows:

① α-Glucosidase structure preparation and finding active sites. The α-glucosidase structure data were obtained from Worldwide Protein Data Bank and then MOE-2015.10 software was applied for the preparation of their 3D structures. A virtual pH of 7 was set to prepare the enzyme molecule structures. The active sites on α-glucosidase were determined using the site finder in MOE by removing all of the water molecules.

② Ligands (inhibitor compounds) preparation. ChemBioOffice 2018 software was applied for preparing the HPC and acarbose structures. These ligand structures were then optimized using the MOE system with the following parameters: force field = MMFF94x; R-Field 1 = 80; cutoff = rigid water molecules; space group p1; cell size = 10, 10, 10; cell shape = 90, 90, 90; and gradient = 0.01 RMS kcal·mol^{-1}A^{-2}. A virtual pH of 7 was set to prepare the ligand molecule structures.

③ Docking performance. The docking investigation was performed on the ligands (HPC and acarbose) and α-glucosidase using MOE-2015.10 software. The RMSD value, DS value, interaction type, amino acid composition, interaction between the amino acid and binding site in α-glucosidase, and the bond distance were collected for analysis.

3.2.5. The Five Lipkin's Rules and ADM Analysis Protocol

A virtual study to investigate the five Lipkin's rules was performed using online software accessed at http://www.scfbioiitd.res.in/software/drugdesign/lipinski.jsp (accessed on 15 March 2023). Some pharmacokinetic parameters were obtained for analysis using the SwissADME web tool (http://www.swissadme.ch/ accessed on 15 March 2023). The output data of the theoretical interpretations of the pharmacokinetic parameters have previously been described [65] and used as public references, which can be accessed online at http://biosig.unimelb.edu.au/pkcsm/theory accessed on 15 March 2023.

3.2.6. Statistical Analysis

All experiments were randomized. The HPG yield and anti-α-glucosidase effect data were analyzed using simple variance. Duncan's multiple range tests and Fisher's LSD tests ($p = 0.05$) were used to compare experiments containing ≥six items and ≤five items, respectively. Statistical Analysis Software version SAS-9.4 (SAS Institute Taiwan Ltd., Taipei, Taiwan) was applied for the statistical analysis in this study.

4. Conclusions

aGIs are considered as an effective treatment for T2D. They have been extensively studied and can be isolated from various natural sources. However, it is quite difficult to obtain a large amount of aGIs from natural sources. Microbial fermentation is a strong tool for producing high yields of various bioactive secondary metabolites, including aGIs. The aim of this study was to establish the fermentation process for the production of a novel anti-glucosidase HPC via fermentation. GNC (a peanut oil processing by-product) was screened as the most suitable substrate for the bioproduction of HPC. This inhibitor compound was used for scaled-up production in a 14 L bioreactor system, resulting in a high-level yield (35.1 μg/mL) when a liquid medium containing 1.25% GNC, 0.075% MgSO$_4$, and 0.0.075% K$_2$HPO$_4$ with an initial pH of 7 was fermented by the TUN03 strain at 30 °C (culture temperature), 250 rpm (shaking speed), and 1.2 vvm (dissolved oxygen content) over 8 h (cultivation time). The HPC was purified and in vitro and docking studies of its bioactivity showed novel antidiabetic enzyme inhibition activity.

Author Contributions: Conceptualization, resources, writing—original draft preparation, and supervision, V.B.N.; methodology, software, validation, data curation, visualization, project administration, and writing—review and editing, V.B.N. and S.-L.W.; formal analysis, V.B.N., S.-L.W. and A.D.N.; investigation, V.B.N. All authors have read and agreed to the published version of the manuscript.

Data Availability Statement: Not applicable.
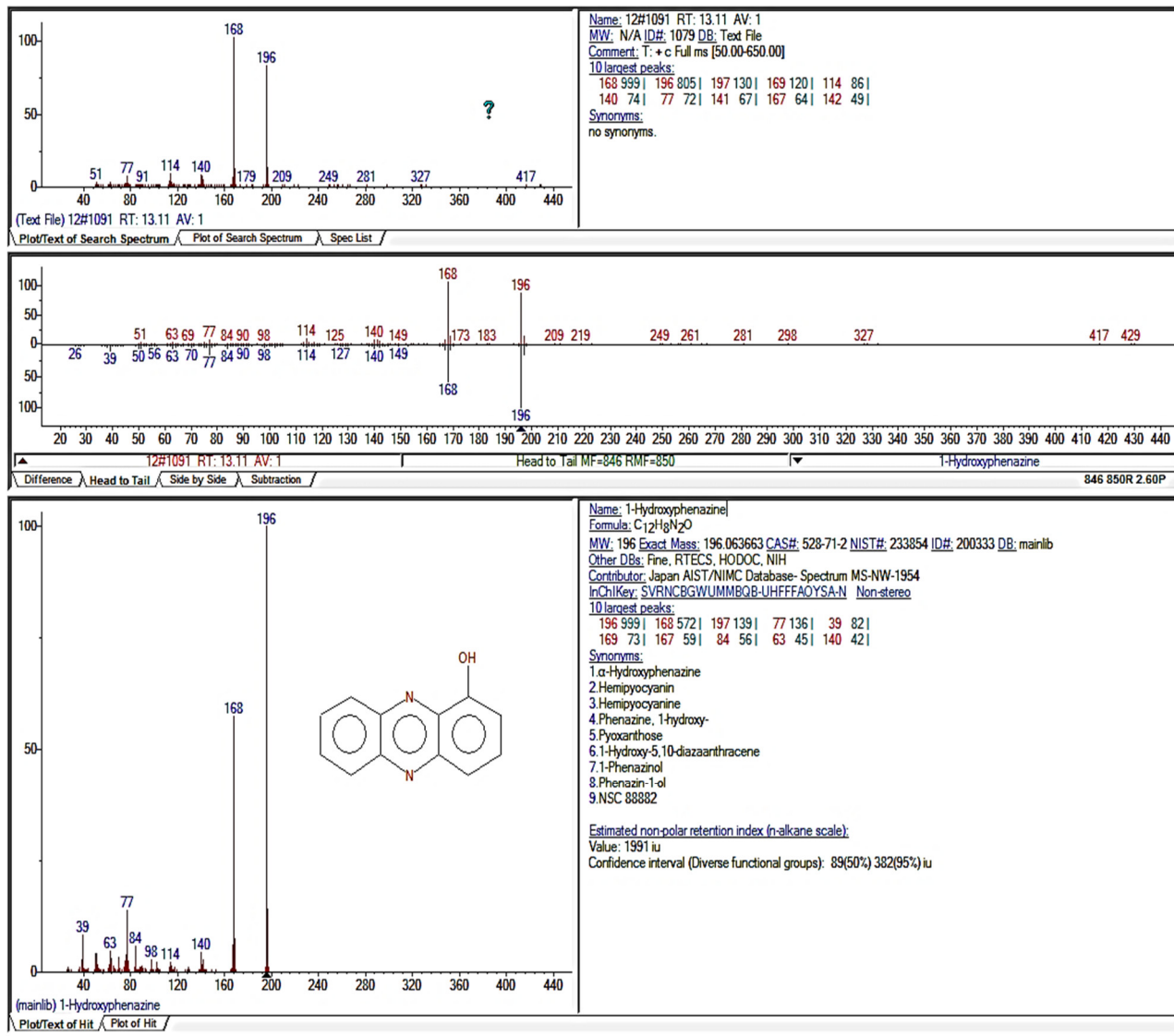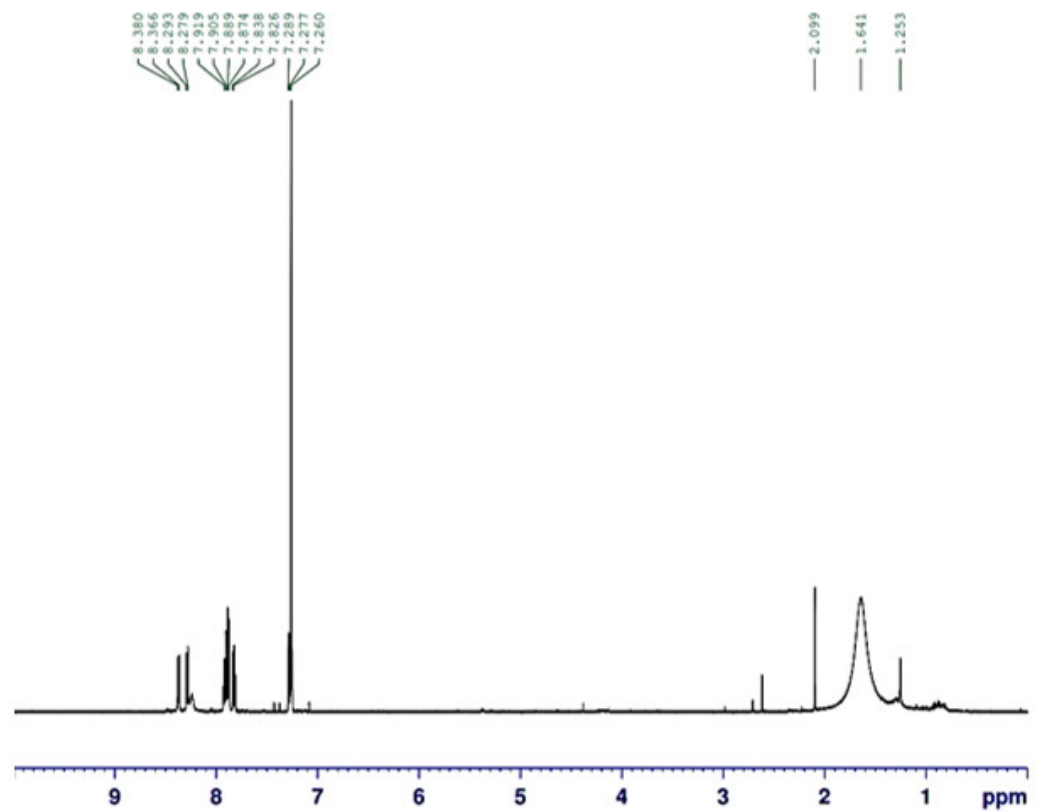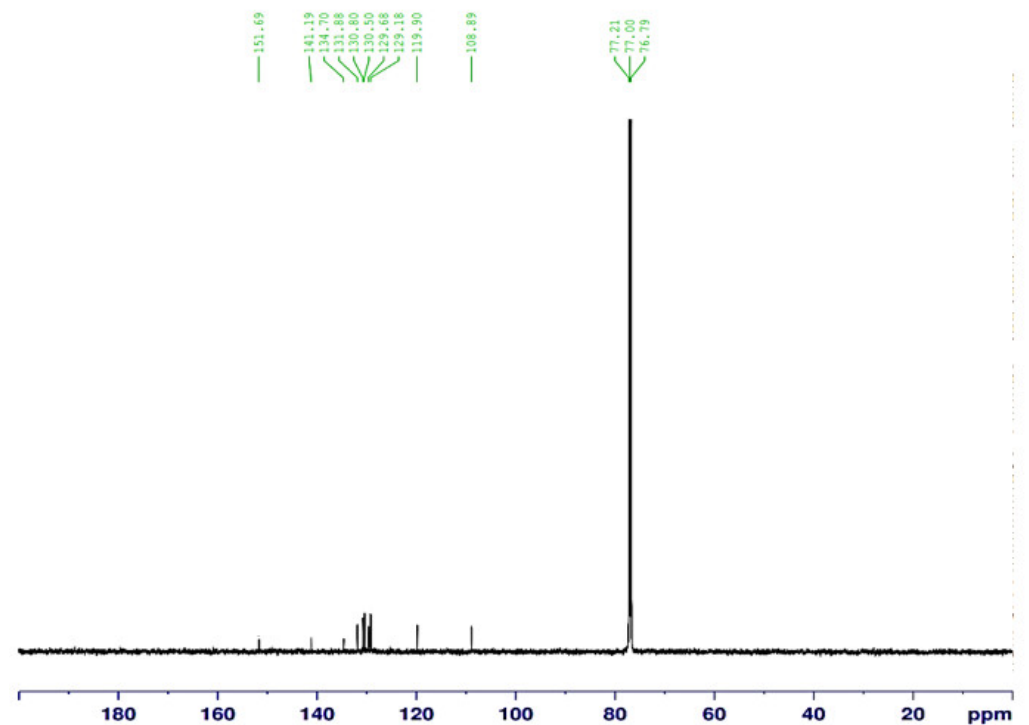
Appendix A

Figure A1. The GCMS analysis of hemi-pyocyanin (also known as 1-hydroxyphenazine).

(a)

(b)

Figure A2. The ^{1}H NMR spectrum (**a**) and ^{13}C NMR spectrum (**b**) of HPC, measured in CDCl$_3$ at 151 MHz and CDCl$_3$ at 600 MHz, respectively.
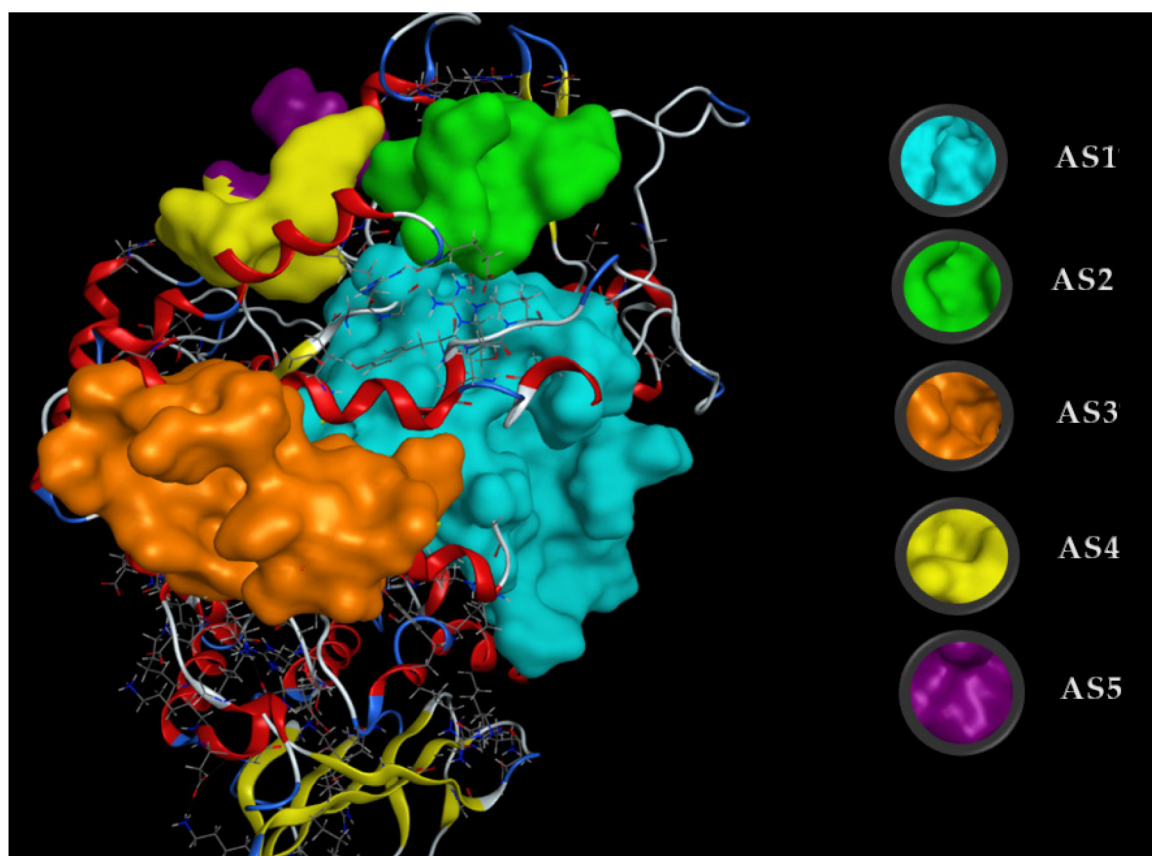
Figure A3. The five active sites (**ASs**) found on α-glucosidase using the site finder function of MOE. The amino acids in **AS1** were ASP69, TYR72, HIS112, LYS156, SER157, TYR158, PHE159, LEU177, PHE178, GLN182, ARG213, ASP215, VAL216, SER240, SER241, ASP242, GLU277, GLN279, HIS280, PHE303, SER304, THR306, ASP307, VAL308, GLY309, THR310, SER311, PRO312, LEU313, PHE314, ARG315, TYR316, VAL319, PRO320, PHE321, ASP325, HIS351, ASP352, GLN353, GLU411, ARG442, and ARG446, those in **AS2** were ASP133, PHE135, PHE136, TRP137, ARG138, and ASN186, those in **AS3** were TRP15, ASN259, GLN260, ILE262, ARG263, VAL266, GLY269, ARG270, GLU271, ILE272, MET273, THR274, TYR289, THR290, SER291, ALA292, ARG294, HIS295, GLU296, LEU297, and SER298, those in **AS4** were ASN76, TYR77, GLU78, HIS117, TRP119, and SER199, and those in **AS5** were ASP64, ALA75, ASN76, GLU116, HIS117, and GLU118.

Table A1. The ADMET-based pharmacokinetics and pharmacology of hemi-pyocyanin and acarbose.

Property	Hemi-Pyocyanin	Acarbose	Unit
Absorption			
Water solubility	−3.06	−1.48	log mol·L^{-1}
Caco2 permeability	1.32	−0.48	log Papp (10^{-6} cm·s^{-1})
Intestinal absorption (human)	95.89	4.17	%
Skin permeability	−2.30	−2.74	log Kp
P-glycoprotein substrate	Yes	Yes	Yes/No
P-glycoprotein I inhibitor	No	No	Yes/No
P-glycoprotein II inhibitor	Yes	No	Yes/No
Distribution			
VDss (human)	−0.17	−0.84	log L·kg^{-1}
Fraction unbound (human)	0.18	0.51	log L·kg^{-1}
BBB permeability	0.38	−1.72	log BB
CNS permeability	−1.74	−6.44	log PS

Table A1. *Cont.*

Property	Hemi-Pyocyanin	Acarbose	Unit
Metabolism			
CYP2D6 substrate	No	No	Yes/No
CYP3A4 substrate	Yes	No	Yes/No
CYP1A2 inhibitor	Yes	No	Yes/No
CYP2C19 inhibitor	No	No	Yes/No
CYP2C9 inhibitor	No	No	Yes/No
CYP2D6 inhibitor	No	No	Yes/No
CYP3A4 inhibitor	No	No	Yes/No
Excretion			
Total clearance	0.60	0.43	$\log \text{mL}\cdot\text{min}^{-1}\cdot\text{kg}^{-1}$
Renal OCT2 substrate	No	No	Yes/No
Toxicity			
AMES toxicity	Yes	No	Yes/No
Max. tolerated dose (human)	0.02	0.44	$\log \text{mg}\cdot\text{kg}^{-1}\cdot\text{day}^{-1}$
hERG I inhibitor	No	No	Yes/No
hERG II inhibitor	No	Yes	Yes/No
Oral rat acute toxicity (LD50)	1.80	2.45	$\text{mol}\cdot\text{kg}^{-1}$
Oral rat chronic toxicity (LOAEL)	2.16	5.32	$\log \text{mg}\cdot\text{kg}^{-1}\_\text{bw}\cdot\text{day}^{-1}$
Hepatotoxicity	No	No	Yes/No
Skin sensitization	No	No	Yes/No
T. Pyriformis toxicity	0.96	0.29	$\log \mu\text{g}\cdot\text{L}^{-1}$
Minnow toxicity	0.68	16.82	$\log \text{mM}$

References

1. Amran, M.A.; Palaniveloo, K.; Fauzi, R.; Satar, N.M.; Mohidin, T.B.M.; Mohan, G.; Razak, S.A.; Arunasalam, M.; Nagappan, T.; Sathiya Seelan, J.S. Value-added metabolites from agricultural waste and application of green extraction techniques. *Sustainability* **2021**, *13*, 11432. [CrossRef]
2. Bala, S.; Garg, D.; Sridhar, K.; Inbaraj, B.S.; Singh, R.; Kamma, S.; Tripathi, M.; Sharma, M. Transformation of agro-waste into value-added bioproducts and bioactive compounds: Micro/nano formulations and application in the agri-food-pharma sector. *Bioengineering* **2023**, *10*, 152. [CrossRef] [PubMed]
3. Esra, C.; Elifsu, N.; Francisco, T.B. Novel approaches in the valorization of agricultural wastes and their applications. *J. Agric. Food Chem.* **2022**, *70*, 6787–6804.
4. Nguyen, T.H.; Wang, S.L.; Nguyen, V.B. Recent advances in eco-friendly and scaling-up bioproduction of prodigiosin and its potential applications in agriculture. *Agronomy* **2022**, *12*, 3099. [CrossRef]
5. Varshney, R.K.; Pandey, M.K.; Puppala, N. The peanut genome, economic and academic importance of peanut. In *Compendium of Plant Genomes*; Chittaranjan, K.M., Ed.; Springer: Berlin/Heidelberg, Germany, 2017; Chapter 2, pp. 7–26.
6. Production Share of Peanuts Worldwide in 2019, by Leading Country. Available online: https://www.statista.com/statistics/1030846/major-producers-of-peanut-worldwide/ (accessed on 4 November 2021).
7. Worldwide Oilseed Production in 2020/2021, by Type. Available online: https://www.statista.com/statistics/267271/worldwide-oilseed-production-since-2008/ (accessed on 16 November 2021).
8. Nautiyal, P.C.; Mejia, D. *Groundnut Post-Harvest Operations*; Food and Agriculture Organization of the United Nations: Rome, Italy, 2002; pp. 1–115.
9. Purohit, C.; Rajyalakshmi, P. Quality of products containing defatted groundnut cake flour. *J. Food Sci. Technol.* **2011**, *48*, 26–35. [CrossRef]
10. Nguyen, T.H.; Wang, S.L.; Doan, M.D.; Nguyen, T.H.; Tran, T.H.T.; Tran, T.N.; Doan, C.T.; Ngo, V.A.; Ho, N.D.; Do, V.C.; et al. Utilization of by-product of groundnut oil processing for production of prodigiosin by microbial fermentation and its novel potent anti-nematodes effect. *Agronomy* **2022**, *12*, 41. [CrossRef]
11. Bhagwat, A.; Padalia, U. Optimization of prodigiosin biosynthesis by *Serratia marcescens* fusing unconventional bioresources. *J. Genet. Eng. Biotechnol.* **2020**, *18*, 26. [CrossRef]
12. Paithankar, A.; Rewatkar, A. Oil cakes as substrate for improved lipase production in solid state fermentation. *IOSR J. Pharm. Biol. Sci.* **2014**, *9*, 31–38. [CrossRef]
13. Gerstein, H.C.; Miller, M.E.; Byington, R.P.; Goff, J.D.C.; Bigger, J.T.; Buse, J.B.; Cushman, W.C.; Genuth, S.; Ismail-Beigi, F.; Grimm, J.R.H. Effects of intensive glucose lowering in type 2 diabetes. *N. Engl. J. Med.* **2008**, *358*, 2545–2559.
14. Ley, S.H.; Hamdy, O.; Mohan, V.; Hu, F.B. Prevention and management of type 2 diabetes: Dietary components and nutritional strategies. *Lancet* **2014**, *383*, 1999–2007. [CrossRef]

15. DeMelo, E.B.; Gomes, A.; Carvalha, I. α-and β-Glucosidase inhibitors: Chemical structure and biological activity. *Tetrahedron* **2006**, *62*, 10277–10302.
16. Nguyen, V.B.; Wang, S.L.; Nguyen, T.H.; Nguyen, M.T.; Doan, C.T.; Tran, T.N.; Lin, Z.H.; Nguyen, Q.V.; Kuo, Y.-H.; Nguyen, A.D. Novel potent hypoglycemic compounds from *Euonymus laxiflorus* Champ. and their effect on reducing plasma glucose in an ICR mouse model. *Molecules* **2018**, *23*, 1928. [CrossRef]
17. Huang, H.T.; Wang, S.L.; Nguyen, V.B.; Kuo, Y.H. Isolation and identification of potent antidiabetic compounds from *Antrodia cinnamomea*—An edible Taiwanese mushroom. *Molecules* **2018**, *23*, 2864. [CrossRef]
18. Dirir, A.M.; Daou, M.; Yousef, A.F.; Yousef, L.F. A review of alpha-glucosidase inhibitors from plants as potential candidates for the treatment of type-2 diabetes. *Phytochem. Rev.* **2021**, *21*, 1049–1079. [CrossRef]
19. Nguyen, V.B.; Wang, S.L.; Nhan, N.T.; Nguyen, T.H.; Nguyen, N.P.D.; Nghi, D.H.; Cuong, N.M. New records of potent in-vitro antidiabetic properties of *Dalbergia tonkinensis* heartwood and the bioactivity-guided isolation of active compounds. *Molecules* **2018**, *23*, 1589. [CrossRef]
20. Chen, J.; Cheng, Y.Q.; Yamaki, K.; Li, L.T. Anti-α-glucosidase activity of Chinese traditionally fermented soybean (dou-chi). *Food Chem.* **2007**, *103*, 1091–1096. [CrossRef]
21. Nguyen, V.B.; Nguyen, A.D.; Kuo, Y.H.; Wang, S.L. Biosynthesis of α-glucosidase inhibitors by a newly isolated bacterium, *Paenibacillus* sp. TKU042 and its effect on reducing plasma glucose in a mouse model. *Int. J. Mol. Sci.* **2017**, *18*, 700. [CrossRef]
22. Fujita, H.; Yamagami, T.; Ohshima, K. Long-term ingestion of touchi-extract, a α-glucosidase inhibitor, by borderline and mild type-2 diabetic subjects is safe and significantly reduces blood glucose levels. *Nutr. Res.* **2003**, *23*, 713–722. [CrossRef]
23. Nguyen, V.B.; Wang, S.L. New novel α-glucosidase inhibitors produced by microbial conversion. *Process Biochem.* **2018**, *65*, 228–232. [CrossRef]
24. Wang, S.L.; Liang, T.W.; Yen, Y.H. Bioconversion of chitin-containing wastes for the production of enzymes and bioactive materials. *Carbohydr. Polym.* **2011**, *84*, 732–742. [CrossRef]
25. Nguyen, V.B.; Nguyen, D.N.; Wang, S.-L. Microbial reclamation of chitin and protein-containing marine by-products for the production of prodigiosin and the evaluation of its bioactivities. *Polymers* **2020**, *12*, 1328. [CrossRef] [PubMed]
26. Sorensen, R.U.; Joseph, F., Jr. Phenazine pigments in *Pseudomonas aeruginosa* infection. In *Pseudomonas aeruginosa as an Opportunistic Pathogen*; Springer: Boston, MA, USA, 1993; pp. 43–57. Available online: https://link.springer.com/chapter/10.1007/978-1-4615-3036-7_3 (accessed on 18 April 2023).
27. Cimmino, A.; Evidente, A.; Mathieu, V.; Andolfi, A.; Lefranc, F.; Kornienko, A.; Kiss, R. Phenazines and cancer. *Nat. Prod. Rep.* **2012**, *29*, 487. [CrossRef] [PubMed]
28. Mavrodi, D.V.; Blankenfeldt, W.; Thomashow, L.S. Phenazine compounds in fluorescent *Pseudomonas* spp. biosynthesis and regulation. *Annu. Rev. Phytopathol.* **2006**, *44*, 417–445. [CrossRef] [PubMed]
29. Liu, H.; He, Y.; Jiang, H.; Peng, H.; Huang, X.; Zhang, X.; Linda, S.T.; Xu, Y. Characterization of a phenazine-producing strain *Pseudomonas chlororaphis* GP72 with broad-spectrum antifungal activity from green pepper rhizosphere. *Curr. Microbiol.* **2007**, *54*, 302–306. [CrossRef] [PubMed]
30. Nikolaus, G.; Wulf, B.; Rolf, B. Recent developments in the isolation, biological function, biosynthesis, and synthesis of phenazine natural products. *Bioorg. Med. Chem.* **2017**, *25*, 6149–6166.
31. Liu, T.T.; Ye, F.C.; Pang, C.P.; Yong, T.Q.; Tang, W.D.; Xiao, J.; Shang, C.H.; Lu, Z.J. Isolation and identifcation of bioactive substance 1-hydroxyphenazine from *Pseudomonas aeruginosa* and its antimicrobial activity. *Lett. Appl. Microbiol.* **2020**, *71*, 303–310. [CrossRef]
32. Alka, R.; Wamik, A. An overview on biosynthesis and applications of extracellular pyocyanin pigment and its role in *Pseudomonas aeruginosa* pathogenesis. *Ann. Phytomedicine* **2019**, *8*, 28–42.
33. Nguyen, T.H.; Wang, S.L.; Nguyen, A.D.; Doan, M.D.; Tran, T.N.; Doan, C.T.; Nguyen, V.B. Novel α-Amylase inhibitor hemi-pyocyanin produced by microbial conversion of chitinous discards. *Mar. Drugs* **2022**, *20*, 283. [CrossRef]
34. Jonathan, O.I. Performance and economic analysis of cockerel chicks fed enzyme supplemented brewer's dried grains groundnut cake-based diets. *Agric. Biol. J. N. Am.* **2011**, *51*, 2151–7517.
35. Nguyen, T.H.; Wang, S.L.; Nguyen, D.N.; Nguyen, A.D.; Nguyen, T.H.; Doan, M.D.; Ngo, V.A.; Doan, C.T.; Kuo, Y.H.; Nguyen, V.B. Bioprocessing of marine chitinous wastes for the production of bioactive prodigiosin. *Molecules* **2021**, *26*, 3138. [CrossRef]
36. Barakat, K.M.; Mattar, M.Z.; Sabae, S.Z.; Darwesh, O.M.; Hassan, S.H. Production and characterization of bioactive pyocyanin pigment by marine *Pseudomonas aeruginosa* Osh1. *Res. J. Pharm. Biol. Chem. Sci.* **2015**, *6*, 933–943.
37. Devnath, P.; Uddin, M.K.; Ahmed, F.; Hossain, M.T.; Manchur, M.A. Extraction, purification and characterization of pyocyanin produced by *Pseudomonas aeruginosa* and evaluation for its antimicrobial activity. *Int. Res. J. Biol. Sci.* **2017**, *6*, 1–7.
38. Ozdal, M.; Gurkok, S.; Ozdal, O.G.; Kurbanoglu, E.B. Enhancement of pyocyanin production by *Pseudomonas aeruginosa* via the addition of n-hexane as an oxygen vector. *Biocatal. Agric. Biotechnol.* **2019**, *22*, 101365. [CrossRef]
39. Ozdal, M. A new strategy for the efficient production of pyocyanin, a versatile pigment, in *Pseudomonas aeruginosa* OG1 via toluene addition. *3 Biotech* **2019**, *9*, 370. [CrossRef]
40. Elbargisy, R.M. Optimization of nutritional and environmental conditions for pyocyanin production by urine isolates of *Pseudomonas aeruginosa*. *Saudi J. Biol. Sci.* **2021**, *28*, 993–1000. [CrossRef] [PubMed]
41. El-Fouly, M.Z.; Sharaf, A.M.; Shahin, A.A.M.; El-Bialy, H.A.; Omara, A.M.A. Biosynthesis of pyocyanin pigment by *Pseudomonas aeruginosa*. *J. Radiat. Res. Appl. Sci.* **2015**, *8*, 36–48. [CrossRef]

42. DeBritto, S.; Gajbar, T.D.; Satapute, P.; Lalitha, S.; Ramachandra, Y.L.; Sudisha, J.; Shin-ichi, I. Isolation and characterization of nutrient dependent pyocyanin from *Pseudomonas aeruginosa* and its dye and agrochemical properties. *Sci. Rep.* **2020**, *10*, 1542. [CrossRef]

43. Hüseyin, K.; Cennet, C.K. Pyocyanine production, twitching motility and hydrophobicity of different wastes on *Pseudomonas aeruginosa*. *Pol. J. Environ. Stud.* **2021**, *30*, 1641–1645.

44. Francisco, J.B.V.; Jesús, A.P.G.; Mayra, L.F.M.; Fabricio, E.A.; Luis, A.O.F.; Yolanda, R.V. Optimized production of a redox metabolite (pyocyanin) by *Pseudomonas aeruginosa* NEJ01R using a maize by-product. *Microorganisms* **2020**, *8*, 1559.

45. Bianca, T.M.O.; Patrik, S.Z.B.; Thiago, G.C.; Ian, P.G.A.; Ulrich, V. Craft beer waste as substrate for pyocyanin synthesis. *IOSR-JPBS* **2019**, *14*, 21–25.

46. Onbasli, D.; Aslim, A. Determination of antimicrobial activity and production of some metabolites by *Pseudomonas aeruginosa* B1 and B2 in sugar beet molasses. *Afr. J. Biotechnol.* **2008**, *7*, 4614–4619.

47. Baron, A.D. Postprandial hyperglycaemia and α-glucosidase inhibitors. *Diabetes Res. Clin. Pract.* **1998**, *40*, 51–55. [CrossRef] [PubMed]

48. Geng, P.; Bai, G. Two novel aminooligosaccharides isolated from the culture of *Streptomyces coelicoflavus* ZG0656 as potent inhibitors of α-amylase. *Carbohydr. Res.* **2008**, *343*, 470–476. [CrossRef] [PubMed]

49. Kim, K.T.; Rioux, L.E.; Turgeon, S.L. Alpha-amylase and alpha-glucosidase inhibition is differentially modulated by fucoidan obtained from *Fucus vesiculosus* and *Ascophyllum nodosum*. *Phytochemistry* **2014**, *98*, 27–33. [CrossRef] [PubMed]

50. McFarland, A.J.; Anoopkumar, D.S.; Perkins, A.V.; Davey, A.K.; Grant, G.D. Inhibition of autophagy by 3-methyladenine protects 1321N1 astrocytoma cells against pyocyanin- and 1-hydroxyphenazine-induced toxicity. *Arch. Toxicol.* **2012**, *86*, 275–284. [CrossRef]

51. Prabhu, M.S.; Walawalkar, Y.D.; Furtado, I. Purification and molecular and biological characterisation of the 1-hydroxyphenazine, produced by an environmental strain of *Pseudomonas aeruginosa*. *World J. Microbiol. Biotechnol.* **2014**, *30*, 3091–3099. [CrossRef]

52. Kerr, J.R.; Taylor, G.W.; Rutman, A.; Høiby, N.; Cole, P.J.; Wilson, R. *Pseudomonas aeruginosa* pyocyanin and 1-hydroxyphenazine inhibit fungal growth. *J. Clin. Pathol.* **1999**, *52*, 385–387. [CrossRef]

53. Kanda, S.; Wirach, W.; Chanokporn, P.; Chalerm, R. Isolation and analysis of antibacterial substance produced from *P. aeruginosa* TISTR 781. *KKU Sci. J.* **2009**, *37*, 163–172.

54. Dharni, S.; Alam, M.; Kalani, K.; Abdul, K.; Samad, A.; Srivastava, S.K.; Patra, D.D. Production, purification, and characterization of antifungal metabolite from *Pseudomonas aeruginosa* SD12, a new strain obtained from tannery waste polluted soil. *J. Microbiol. Biotechnol.* **2012**, *22*, 674–683. [CrossRef]

55. Xiao, J.; Thwe, A.A.; Liu, T.T.; Dafei, G.; Wanhua, L.; Changhua, S.; Lu, S.J. Anti-inflammatory effects of an extract from *Pseudomonas aeruginosa* and its purified product 1-hydroxyphenazine on RAW264.7 cells. *Curr. Microbiol.* **2021**, *78*, 2762–2773. [CrossRef]

56. Ding, Y.; Fang, Y.; Moreno, J.; Ramanujam, J.; Jarrell, M.; Brylinski, M. Assessing the similarity of ligand binding conformations with the contact mode score. *Comput. Biol. Chem.* **2016**, *64*, 403–413. [CrossRef]

57. Chandra, B.T.M.; Rajesh, S.S.; Bhaskar, B.V.; Devi, S.; Rammohan, A.; Sivaraman, T.; Rajendra, W. Molecular docking, molecular dynamics simulation, biological evaluation and 2D QSAR analysis of flavonoids from *Syzygium alternifolium* as potent anti-Helicobacter pylori agents. *RSC Adv.* **2017**, *7*, 18277–18292. [CrossRef]

58. Kim, Y.; Wang, M.; Rhee, M.J. A novel alpha-glucosidase inhibitor from pine bark. *Carbohydr. Res.* **2004**, *339*, 715–717. [CrossRef]

59. Oko, J.O.; Abriba, C.; Audu, J.A.; Kutman, N.A.; Okeh, Q. Bacteriological and nutritional analysis of groundnut cake sold in an open market in Samaru, Zaria-Kaduna State. *Int. J. Sci. Technol. Res.* **2015**, *4*, 225–228.

60. Señoráns, F.J.; Luna, P. Sample preparation techniques for the determination of fats in food. *Compr. Sampl. Sample Preparat.* **2012**, *4*, 203–211.

61. Dubois, M.; Gilles, K.A.; Hamilton, J.K.; Rebers, P.A.; Smith, F. Colorimetric method for determination of sugars and related substances. *Anal. Chem.* **1956**, *28*, 350–356. [CrossRef]

62. Miller, G.L. Use of dinitrosalicylic acid reagent for determination of reducing sugar. *Anal. Chem.* **1959**, *31*, 426–428. [CrossRef]

63. Nguyen, V.B.; Nguyen, A.D.; Wang, S.L. Utilization of fishery processing by-product squid pens for α-glucosidase inhibitors production by *Paenibacillus* sp. *Mar. Drugs* **2017**, *15*, 274. [CrossRef]

64. Tran, L.T.; Techato, K.; Nguyen, V.B.; Wang, S.-L.; Nguyen, A.D.; Phan, T.Q.; Doan, M.D.; Phoungthong, K. Utilization of cassava wastewater for low-cost production of prodigiosin via *Serratia marcescens* TNU01 fermentation and its novel potent α-glucosidase inhibitory effect. *Molecules* **2021**, *26*, 6270. [CrossRef]

65. Pires, D.E.; Blundell, T.L.; Ascher, D.B. PkCSM: Predicting smallmolecule pharmacokinetic and toxicity properties using graphbased signatures. *J. Med. Chem.* **2015**, *58*, 4066–4072. [CrossRef]